Proceedings of the CAS–CERN Accelerator School: Free Electron Lasers and Energy Recovery Linacs, Hamburg, Germany, 31 May–10 June 2016, edited by R. Bailey, CERN Yellow Reports: School Proceedings, Vol. 1/2018, CERN-2018-001-SP (CERN, Geneva, 2018)

Beam Dynamics of Energy Recovery Linacs

A. Jankowiak, M. Abo-Bakr, and A. Matveenko
Helmholtz-Zentrum Berlin, Germany

Abstract

Energy recovery linacs (ERLs) combine the advantages of the two major accelerator types used at present: the high currents and low energy consumption of storage rings and the rapidly accelerated, high-brilliance beams of linear accelerators (linacs). As concepts from both accelerator types are adopted, similar beam physics challenges need to be overcome in the design of an ERL. In the first part of this article we describe the main requirements and layout options for an ERL's beam optics, pointing out the individual demands of the various subparts of the ERL: injector, merger and splitter, linac section, and recirculator. In the second part, collective high-current effects are introduced with a focus on space charge, coherent synchrotron radiation, the microbunching instability, and beam break-up. A comprehensive list of references is given for readers interested in further details of the topics introduced.

Keywords

ERL; beam dynamics; optics; collective effects.

1 Introduction

Energy recovery linacs (ERLs) can generate high-energy electron beams of huge virtual power and high density, and thus it is possible to base a synchrotron radiation light source of the ultimate brightness on them. Short pulses and high peak currents will also allow the generation of coherent radiation. Although terahertz radiation can be emitted from short bunches, low-gain free-electron laser (FEL) operation (i.e., an FEL amplifier) is also possible. Even high-gain FEL operation is feasible, as long as the beam degradation remains within the machine acceptance (transverse and momentum). Another application option is to use an ERL as a Compton source, generating hard X-rays from low-energy electrons.

In storage rings, the beam dimensions result from an equilibrium state between radiation excitation and damping, and hence are totally independent of the quality of the beam from the source, and totally independent of all pre-accelerators. In ERLs, as they are single- or few-turn machines, the passage time is much too short to reach this equilibrium and the beam quality is defined by the electron source. Whereas for a given storage ring the emittance ε scales as $\varepsilon \sim E^2$, in ERLs adiabatic damping causes an $\varepsilon \sim E^{-1}$ scaling. Thus, with increasing energy, the bunch quality in an ERL improves. Using present-day high-brightness electron sources, based on laser-induced photoemission from a gun cathode, ERLs have the potential to significantly exceed the bunch quality of modern storage-ring-based, third-generation light sources. The physics of these sources is a large topic of its own and will not be covered here [1, 2].

The central goal parameter for almost all kinds of present and future accelerators, and especially for synchrotron radiation light sources, is the brilliance $B \sim N/\varepsilon_x\varepsilon_y$, which scales with the number of electrons per second N and the transverse emittances ε_x and ε_y. Small emittances of bunches with a high charge and a high repetition rate maximize the average brilliance. Short pulses from ERLs enable insights into the dynamics of subpicosecond processes and can produce an extreme peak brilliance $\hat{B} \sim B/\sigma_s$. The spectral brilliance obtained from long insertion devices scales inversely with the energy spread, i.e., $B(\omega) \sim 1/\sigma_E$. Thus achieving the ultimate spectral brilliance, average as well as peak, requires beams of the highest electron densities, not only in 3D but also in the six-dimensional phase space.

As ERLs can reach and exceed storage ring beam parameters in any phase space dimension, many of the beam dynamics challenges known for storage rings are relevant to ERLs as well and can affect

https://doi.org/10.23730/CYRSP-2018-001.439

their performance, possibly even to a higher degree. The beam dynamics challenges in an ERL arise from its general layout and target parameters, and vary with beam energy and with the function of the various machine sections.

- *Injector.* This provides high-brightness beam generation and low-energy beam transport under the influence of strong space charge forces.
- *Merger.* This guides both the low-energy fresh beam and the high-energy used beam into the same linac section.
- *Linac section(s).* This provides acceleration and deceleration of the beam. Depending on the target energy, available linac length, and average accelerating gradients, a layout based on single linac, a split linac, or a multipass linac can be chosen.
- *Spreader.* Using a multiturn layout, the various beams must be merged into the linac section, and after acceleration/deceleration be sent to beam lines according to their energy.
- *Recirculation section.* This provides lossless beam transport with conserved beam quality, with the option of beam manipulation; variants of arc lattices (Bates, double-bend achromat (DBA), triple-bend achromat (TBA), multi-bend achromat (MBA), and fixed-field alternating-gradient (FFAG)) generate the conditions for the most efficient energy recovery.
- *Splitter and dump line.* This section is analogous to the merger: downstream of the linac section, the fresh and used bunches need to be separated, for further acceleration or light generation with the former and to guide the latter into the dump line.

For this overview report, we separate the beam dynamics issues of ERL-based synchrotron radiation facilities into two main categories:

- *beam optics,* dealing mostly with charge- and current-independent problems of linear and non-linear beam transport, manipulation, and acceleration; and
- *collective effects,* caused by the high electron density and average current, which can degrade the beam quality, drive instabilities, and ultimately even lead to partial or total beam loss.

In the first, 'beam optics' part we will introduce general magnet optics designs applicable to ERLs, and discuss the design philosophies of the subcomponents. The requirements on the beam optics are collected together and the magnet lattice configurations that best satisfy them are compared. Non-linear effects and their compensation by adjusting the linear optics and by the use of higher-order magnetic multipole elements are considered. In the second part, the physics of potentially harmful collective effects is introduced. Options to counteract these effects by the use of special optics settings are discussed.

Since derivations of the fundamental formulas presented here are far beyond the scope of this report, a selection of references to specialized papers is given for each issue considered. In general, the online journal *Physical Review Accelerators and Beams* [3] and the proceedings of the International Particle Accelerator Conference (IPAC) and ERL workshops hosted by JACoW, the Joint Accelerator Conferences Website [4], provide an excellent source of information on all fields of ERL beam dynamics issues. As the authors were involved in the design of two ERL projects, we would like to refer the reader also to the conceptual design reports for these projects, which give a good insight into the beam dynamics aspects of low- and high-energy ERLs: bERLinPro [5, 6], currently under construction at the Helmholtz-Zentrum Berlin (HZB), and FSF, the Femto-Science-Factory [7], an HZB design study for a 6 GeV ERL-based synchrotron light source.

2 Beam optics

The magnetic lattice is defined by the type, number, and arrangement of multipole magnets and radio frequency (RF) structures. These devices are tuned to form a beam optics system, capable of transporting the beam (including acceleration and deceleration) throughout the machine while:

- maintaining the beam quality delivered from the source;
- ensuring minimum electron losses;
- merging or splitting beams of various energies, for example injected and recirculated beam(s);
- performing bunch manipulations, for example compression, emittance exchange, and plane rotation;
- establishing conditions for efficient energy recovery.

There are many challenges related to specific parts of an ERL. In contrast, particle losses and beam size are issues in all machine sections and thus will be covered here first.

2.1 Beam size and losses

In optics simulations, the beam is described by its 6D phase space size $\sigma_x, \sigma_{x'}, \sigma_y, \sigma_{y'}, \sigma_s, \sigma_E$, its emittances $\varepsilon_x, \varepsilon_y, \varepsilon_s$, and its Twiss parameters $\beta_{x,y}, \alpha_{x,y}, \gamma_{x,y}$, assuming Gaussian particle distributions. The behaviour of energy-deviating electrons is described by the dispersion function η. Various partially contradictory demands are made on the beam size.

- For a high-brilliance light source, suitable electron bunches at the point(s) of radiation generation are required. Small beam sizes in all dimensions enable generation of diffraction-limited light pulses with high transverse and longitudinal coherence fractions. For the minimum radiation wavelength λ_γ to be generated, diffraction puts a lower limit on the transverse emittances $\varepsilon_{x,y} \approx \lambda_\gamma/4n$, such that smaller electron beam emittances do not further reduce the photon beam size [8].
- Particle losses are at least as important as they are in storage rings. Although beam decay (as in storage rings) is not an issue, radiation and activation issues, as well as RF power limits, are of great importance. Especially, losses in high-energy turns need to be minimized as far as possible. The beam size is directly involved in two mechanisms:
  - *losses at the machine aperture:* the transverse beam size must be small compared with the dimensions A of the vacuum chamber: $A_{x,y}(s) > N\sigma_{x,y}(s)$. In large storage rings, N is quite high, of order 10^2–10^3, whereas in the lower-energy parts of ERLs this number can be much smaller. In dispersive sections passed through by a chirped beam, N can be of the order of 10 or even below. To reach storage-ring-like relative loss rates of 10^{-10} per turn, one needs $N \geq 7$ for a Gaussian-distributed beam. Starting from the electron source, any emission of electrons into the extreme tails of the distribution must be prevented. Nevertheless, halo electrons independent of any assumed distribution function can contribute to particle losses.
  - *Touschek losses (see Section 2.4):* electron collisions within a bunch (intrabeam scattering) lead to momentum transfer between the transverse and longitudinal motions and can be a source of beam halo formation and losses in ERLs. The loss rate from these Touschek events scales with the electron density and thus with the bunch charge and volume. A low density, i.e., a large bunch volume, reduces Touschek losses.
- Collective effects, for example space charge, coherent synchrotron radiation (CSR), and other kinds of wake fields (see Sections 3.1 and 3.2), act on the beam and imprint an energy modulation along the bunch, which ultimately deteriorates the beam quality. As the strength of all these effects scales with the peak current and thus inversely with the bunch length, bunches should be kept long during transport if possible, and only tuned short when generating radiation.
- RF curvature is important: while passing through the RF structures for acceleration or deceleration, the bunches scan the temporal and spatial field variation in the cavities, generating a correlation in the longitudinal phase space. The non-linear part of this correlation can limit bunch manipulation techniques, for example bunch compression, and increases the energy spread. As short bunches scan a smaller RF phase range, non-linearities are reduced compared with longer bunches.

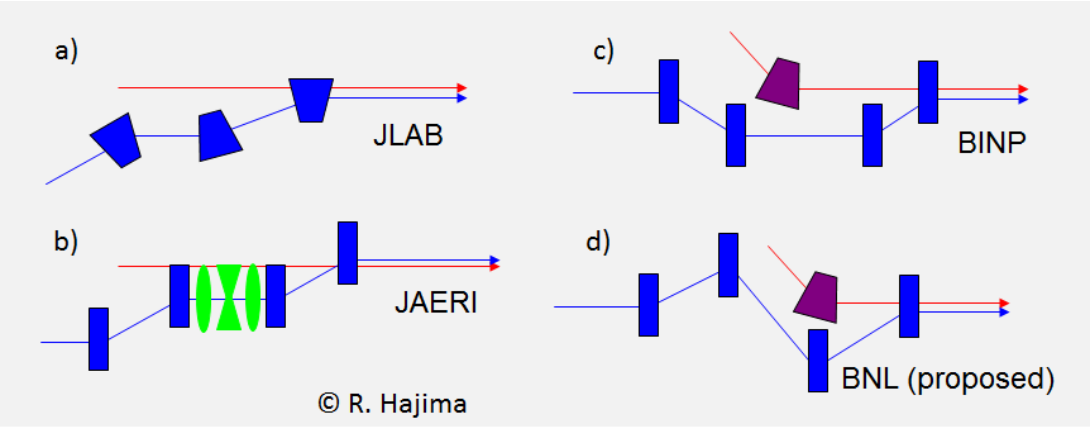

Fig. 1: Mergers for existing and proposed ERLs: (a) deflecting three-bend dog-leg, (b) four-bend dog-leg, (c) four-bend chicane, (d) 'zigzag' merger.

The optimal beam size is a compromise between these demands and has to be found for the various machine sections. Besides the beam size, many more aspects needs to be considered—the most important ones for the various machine sections of an ERL will be covered in the following.

2.2 Injector line and merger

The first machine section, which guides the beam from the source to the first multibeam linac, is referred to as the injection line here. On exit, the low-energy beam must be merged with the high-energy beam to pass through the linac on the same centered trajectory.

Beam transport in the injection line at energies of a few MeV is space charge dominated. Spatially varying forces due to self-generated fields in the bunch can cause significant emittance growth. By following an emittance compensation scheme [9, 10], a sophisticated beam optics system can reverse these space charge effects and cancel the emittance degradation to a major degree. The basic concept is described in Section 3.1. As space charge effects scale strongly with the beam energy, pre-acceleration in the injection line and before the first major acceleration will reduce the initial emittance growth. On the other hand, the pre-acceleration energy is not recovered in an ERL, and RF and dump power considerations will limit its value.

At the end of the injector line, the new and the recirculated beam have to be merged into the linac section. This is achieved by a series of bending magnets, where the last one is passed through by both beams, which are bent at different angles according to their respective energies. Whereas at the beginning of the injector line the optics can be kept axially symmetric and solenoids provide sufficient focusing, the symmetry is broken in the merger. Quadrupole magnets are used here to control dispersion (to form an achromatic bump) and to shape the beam size throughout the merger. Mergers with four different layouts, shown in Fig. 1, have been considered for ERL test facilities [11]: dog-leg-type (Fig. 1(a) and (b)), chicane-type (Fig. 1(c)), and zigzag-type (Fig. 1(d)) mergers.

In contrast to the start of the injection line, in the merger the longitudinal space-charge-induced energy modulation takes place in a dispersive section. Thus, with any energy change, an oscillation around the shifted, new reference path is excited. Since the energy modulation varies along a bunch from its tail to its head, the centroids of longitudinal slices through the bunch oscillate as well. On leaving the merger, the projected emittance in the merger plane can be significantly increased. The emittance growth of parts of the bunch with a linear energy modulation $\Delta E(s) \sim s$ (where s is the longitudinal position in the bunch) can be removed by adjusting the dispersion at the merger exit. When this is done, however,

the achromaticity of the merger is broken, so that variations in the initial energy now cause an emittance growth at the merger exit. Finally, the merger is set up to minimize the overall emittance growth due to space charge dispersion and unclosed merger dispersion ($\eta_x = 0$ m out of the merger).

The same physics applies to the splitter, which divides the accelerated, high-energy beam from the decelerated, low-energy beam, which is sent into the dump line.

Stray fields also need to be considered. Although they are unwanted in general, interfering fields such as the Earth's magnetic field, remanent fields from the optics magnets, and magnetic fields from vacuum pumps and gauges are most distorting in the injection line owing to the low beam energy and low rigidity. Shielding of fields, magnet-cycling procedures, and careful placing of vacuum devices reduce these stray fields. For the remaining fields, trajectory offsets have to be corrected with a sufficient number of steerer magnets.

2.3 Linac sections

One or more ERL sections are equipped with linacs to accelerate the beam in one or several turns up to its final energy. Several aspects of the beam dynamics have to be considered.

- *RF focusing.* The cavity fields focus the beam [12], both horizontally and vertically, when it enters the cavity, and defocus it when it leaves. During acceleration, owing to the energy increase in the cavity, the focusing on the low-energy side prevails over the defocusing on the high-energy side. The opposite effect happens during deceleration. Especially at low energies, the focal strength is high and needs to be carefully considered when the linac section beam optics are being set up.
- *RF phase slip.* At low injection energies, the beam is not sufficiently relativistic and time-of-flight effects can cause a phase slip relative to the recirculated, high-energy beam. A power mismatch in the RF cavities is the consequence, and beam-loading problems arise. The effect can be reduced by increasing the injection energy, but clearly at the cost of the RF and dump power.
- *Multienergy beam lines.* The linac sections are passed through by beams of different energies, sharing the same focusing elements, namely magnets and RF structures. The difficulty of finding suitable optics for all beams scales with the range of energy in the beam line. The optics are mainly tuned with respect to the lowest-energy beam, because it has the lowest magnetic rigidity. Any other strategy would lead to strong overfocusing and an unsuitable beam size. The lack of focusing for the high-energy beam has to be compensated in a separate beam transport section or sections.
- *Spreader.* The separation of the multiple beams into energy-adjusted beam lines is done by a spreader, using the energy dependence of the bending angle in the first, shared dipole magnet(s). The challenge here is to create a compact layout, using a small number of magnets even for several beams of different energies. The dispersion in the spreader plane should be closed at its exit, and the beam size must be matched to the recirculation arcs to avoid emittance degradation.
- *Beam break-up (BBU).* The BBU instability (see Section 3.5) is driven by a positive feedback of the beam into higher-order-mode (HOM) fields of the superconducting RF cavities. Although the most important countermeasure is the use of cavities with a minimized HOM spectrum, the beam optics also influence BBU: a betatron phase advance of $\Delta\psi = n\pi$ between consecutive cavity passages sets the transport matrix element R_{12} to zero, so that the beam passes through the cavity on axis after recirculation and no power is fed into the HOMs (see Eq. (2)). In addition, optimized Twiss parameters for the linac can be calculated [13]. Both of these measures can significantly increase the instability threshold. Effective measures against BBU become even more important for multiturn ERLs, where various beams (multiplying the total current) traverse the linac sections simultaneously.

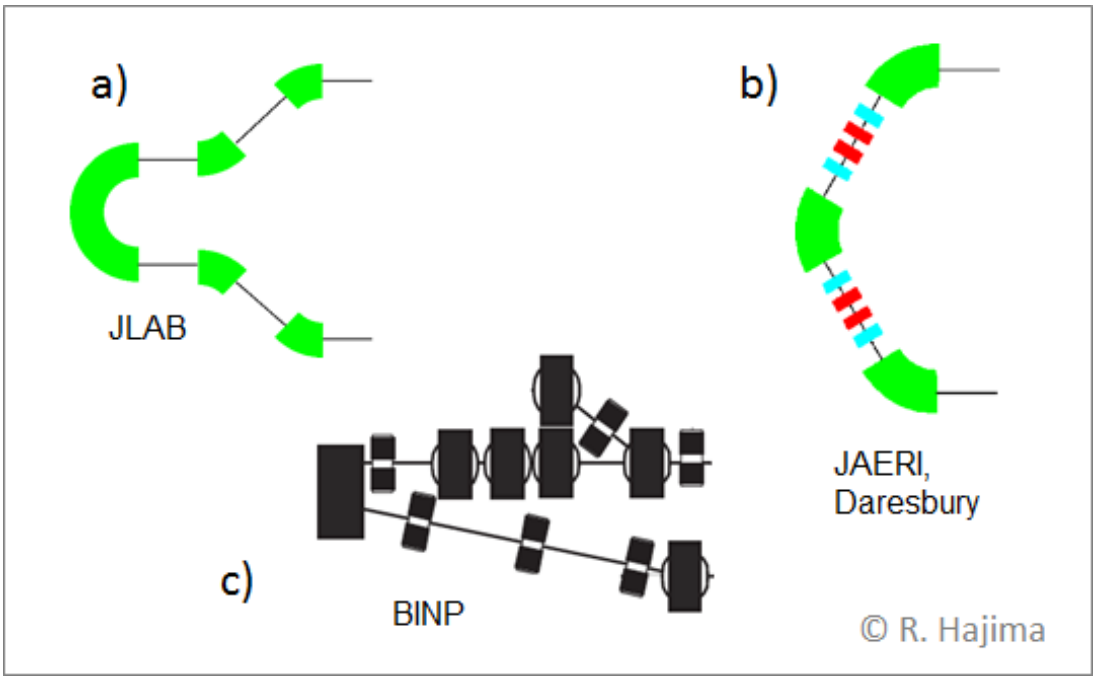

Fig. 2: Recirculator arc lattice types: (a) Bates arc, (b) TBA, (c) BINP arc

2.4 Recirculators

The transfer lines connecting the ERL linac sections and the full-energy section dedicated to radiation generation are referred to here as recirculators. Together with the linac sections, they form the majority of the machine sections in an ERL. A careful beam optics set-up, fulfilling a variety of demands, is mandatory. Several basic lattice concepts are suitable for ERL recirculator arcs, depending on the energy and on the available space and number of magnets [14]. In low- to medium-energy ERLs of moderate size, DBAs [15], TBAs [16], Bates arcs [17], and also individual, non-standard schemes have been applied, as shown in Fig. 2.

For large-scale ERL-based light sources with energies in the GeV range, multibend achromat lattices and FFAG lattices have been considered [18–22]. The various lattice types differ in their tunability, space, and magnet number requirements, and in performance with respect to emittance conservation, lossless beam transport, and beam manipulation capabilities. Flexible control of the linear and non-linear beam optics is the key to covering all of the aspects mentioned above.

2.4.1 Lossless beam transport

As mentioned earlier, Touschek scattering is one of the two dominant loss processes. Besides a large bunch volume, which is contrary to radiation generation requirements, the momentum acceptance A_p of the optics is of crucial significance. Although energy transfer due to intrabeam scattering into the transverse motion is of minor importance, the longitudinal momentum change is Lorentz transformed into the laboratory frame and is thus strongly enhanced. With a momentum change $\Delta p/p$ from a scattering event, the downstream reference trajectory shifts to a dispersive path $x_{\mathrm{ref}}(s) = \eta(s) \cdot \Delta p/p$. Depending on the dispersion function at the scattering position, a betatron oscillation of initial amplitude

$$\begin{pmatrix} x \\ x' \end{pmatrix} = \frac{\Delta p}{p} \begin{pmatrix} \eta \\ \eta' \end{pmatrix}$$

may be excited in addition. This is equivalent to a single-particle emittance of

$$\varepsilon_0 = \gamma x^2 + 2\alpha x x' + \beta x'^2 \quad = \quad (\Delta p/p)^2(\gamma\eta^2 + 2\alpha\eta\eta' + \beta\eta'^2) = (\Delta p/p)^2\mathcal{H}\,, \tag{1}$$

$$\mathcal{H} \;=\; \gamma\eta^2 + 2\alpha\eta\eta' + \beta\eta'^2 \tag{2}$$

(the Twiss parameter, dispersion, and $\mathcal{H}$-function are evaluated at the scattering position $s = s_0$). The general expression for the downstream trajectory of the scattered electrons is

$$x(s) \;=\; \sqrt{\varepsilon_0\beta(s)}\cos\left(\psi(s) - \phi_0\right) + \eta(s)\,\Delta p/p \tag{3}$$

$$\;=\; \Delta p/p\left[\sqrt{\mathcal{H}_0\beta(s)}\cos\left(\psi(s) - \phi_0\right) + \eta(s)\right], \tag{4}$$

which is directly proportional to $\Delta p/p$. Scattering events that cause a downstream offset larger than the available horizontal aperture $A_x(s)$ lead to particle losses. The maximum deviation $\Delta p/p$, where $x(s) = f(\Delta p/p) \leq A_x(s)$, defines the momentum acceptance $A_p(s)$ of the optics. The Touschek loss rate [23] scales as $\dot{N}/N \sim 1/A_p^3$, and therefore a large momentum acceptance is essential for low losses. A small overall dispersion and lower maxima of the beta and dispersion functions optimize the $\mathcal{H}$-function (reducing its maximum value) and thus increase the momentum acceptance (see also Section 3.2). Lattices with lower bending angles of the dipole magnets are advantageous, but require more magnets at increased cost.

The loss rate due to elastic scattering from the atomic nuclei of the residual gas is the second main loss mechanism. The loss rate scales as $\dot{N}/N \sim 1/(\theta_x^2 + \theta_y^2)$, with the angular acceptance $\theta_{x,y}^2 \approx A_{x,y}^2/(\langle\beta_{x,y}\rangle\beta_{x,y}^{\max})$. Smaller transverse beta functions with lower maximum values increase the angular acceptance, thus reducing the loss rate. Besides the intentionally generated 'wanted beam', there are a few sources of unwanted beam, for example stray light from the gun laser, extreme tails of the distribution, ghost pulses, and dark current from field emission from the (superconducting) RF structures. This unwanted beam, often referred to as beam halo, can be simulated if the generating process is known. Unfortunately, the dominating contributor only becomes apparent in the real machine, and may even change its origin. The best measure to control beam halo is a large acceptance of the magnet optics to transport both the core beam and the halo.

2.4.2 Bunch manipulation

To generate the most brilliant light pulses, several manipulation techniques are applied that exchange parts of phase space between two planes by means of quasi-phase-space rotations. Conservation of the uninvolved phase space dimensions and the overall beam quality is mandatory.

In many linear accelerators and ERLs, bunch compression is used, where in the first step a chirp (mostly a linear z–p_z correlation, $\Delta p/p = C \cdot \Delta z$) is imprinted by passing the beam through the RF structures off crest. In the second step, the beam passes through a dispersive section with $\eta \neq 0$, where the path length depends on the particle momentum in accordance with $\Delta L = R_{56}\,\Delta p/p + T_{566}(\Delta p/p)^2 + \ldots$, with $R_{56} = \int \eta/\rho\, ds$ and T_{566} as the first- and second-order beam transport matrix elements. Nonlinearities (RF curvature, T_{566}, etc.) can be corrected using higher-order multipole magnets, starting with sextupole magnets at the lowest order. Whereas extra bunch compressor sections are often provided in linacs, in ERLs the recirculation arcs can be used as an alternative. The various lattice types offer different amounts of variability for tuning the optics: for an achromatic arc ($\eta_{\rm in} = \eta_{\rm out} = 0$), the DBA lattice offers no R_{56} tunability at all, whereas, for example, in a TBA lattice R_{56} can be tuned via the dispersion function of the middle bend. With more quadrupole magnets in the more complex lattice types, one generates 'free knobs' to adjust the dispersion and beta functions for non-linear corrections, minimizing the required multipole strengths. Also, the phase advance in certain sections can be tuned with respect to emittance-degrading effects, for example CSR.

Another manipulation that can be done in ERLs is so-called 'beam rotation', where the two transverse phase spaces are completely switched. This can increase the BBU threshold for polarized cavities, since no further excitation of the kicking HOM occurs on the return pass. A section with a set of skew

quadrupole magnets is required to swap the transverse planes, ideally transforming the beam in accordance with

$$\vec{X_1} = M\vec{X_0}, \qquad \text{with} \qquad M = \begin{bmatrix} 0 & E \\ E & 0 \end{bmatrix}, \quad E = \begin{bmatrix} 1 & 0 \\ 0 & 1 \end{bmatrix}.$$

There are more manipulation techniques, for example emittance exchange, but they have either not been used or not been required in ERLs so far.

2.4.3 Energy recovery

A further important task of recirculator arcs is to provide path length adjustment options, to enable one to set up accurately the required RF phase advances of 0 or 180° between linac sections. Depending on the ERL layout, these tuning options may be needed not only in the deceleration but also possibly in the acceleration pass. Common options are movable arcs for small ERLs with 180° DBA, TBA, or Bates arcs (the latter only in the large centre magnet), two longitudinal movable bends within an arc (e.g., in bERLinPro), or high-amplitude steering bumps in large recirculators with sufficient mechanical aperture. Chicanes outside the recirculators can also be used, but they can significantly contribute to the R_{56} budget and can only lengthen the pass (compared with the straight option with all bends off). Moreover, a lengthening of the order of the RF wavelength with a chicane requires large offsets and is hard to achieve in a single wide vacuum chamber.

Beam matching, especially in the last deceleration to the lowest energy, is of vital importance for the efficiency of the recovery process. Minimization of the energy spread at the low-energy side is a precondition for a high recovery rate and for safe transport of the high-power beam into the dump. One option to cancel out RF curvature effects is to adjust the bunch length so that it is equal to that during acceleration. In this case, any bunch compression needs to be reversed. Owing to beam-loading effects, this can be only done by inverting the sign of R_{56} in the corresponding recirculator sections, which again favours highly tunable lattice types with a wide range of values of R_{56}. If the bunch length differs between acceleration and deceleration, sextupole magnets can be used to remove RF non-linearities. Any remaining non-linearities arising from the magnet optics or from collective effects (CSR, wakes, ...) have to be minimized using higher-order multipole magnets.

For efficient recovery, the transverse beam size in the linac needs to be adjusted to take RF focusing into account and also to provide suitable BBU conditions.

2.4.4 Radiation excitation

Despite the transfer line character of ERLs and the short passage times, the emission of incoherent synchrotron radiation (ISR) can cause considerable emittance growth. Since the energy loss due to emission of synchrotron radiation scales as $\Delta E \sim E^4/\rho \sim E^3 B$, high-energy ERLs are most affected. Moreover, the critical photon energy ε_c scales non-linearly with energy, as $\varepsilon_c \sim E^3/\rho \sim E^2 B$, extending the photon spectrum equivalently to higher values, and thus increasing the resulting energy change and energy spread of the emitting electrons. Similarly to a Touschek event, an energy change in a dispersive section excites a betatron oscillation around the new reference orbit. The corresponding emittance growth is described by the function $\mathcal{H}$ (see Eq. (1)), which relates the momentum change to the amplitude of the downstream transverse betatron oscillations. A low $\mathcal{H}$-function represents an optics system where momentum changes cause a smaller transverse-phase-space blow-up and thus reduced emittance growth. Assuming an achromatic arc tuning, minimal form factors $F \sim \mathcal{H}$ can be calculated for the various lattice types for comparison [24]. Compared with the DBA lattice, the theoretical minimum for an MBA lattice is reduced by a factor of 3 when the Twiss parameters and the dispersion function are optimized to reduce $\mathcal{H}$ and extra bends at the beginning and end of the cell close the dispersion. Thus, the emittance growth will be smaller with an MBA lattice, but zero-dispersion sections, for example for insertion devices, are not available without lattice modifications.

2.5 Dump line and beam dump

The ERL's last section is the dump line, which guides the low-energy but high-power beam into the beam dump, where sufficient cooling power is provided to safely absorb the beam in the walls. Losses in the dump line are no longer relevant for the RF budget, but the high-power beam has substantial damage potential. When mis-steered, the beam is able to melt holes in vacuum chamber components on a very short timescale. Thus lossless beam transport is the main task of the beam optics. Large apertures are essential, therefore, to allow safe beam transport with increased emittance (compared with that in the injector) and a moderate further emittance degradation due to space charge effects in the dump line.

In the dump, the full beam power of hundreds of kilowatts or even megawatts is mostly transferred into heat (and radiation). Clearly, this must not happen in an area of a few square millimetres or less, not even an area of a few square centimetres. Instead, the beam power needs to be carefully distributed over the inner surface of the dump, usually over an area of the order of 1–2 m^2. Two options exist:

- beam widening by massively increasing (by orders of magnitude) the beta functions in the last part of the dump line and in the dump;
- beam sweeping using two rapid-cycling (at tens of hertz) transverse steerers, to distribute equally the beam impact points in the dump.

Ideally, a combination of both is used to relax the hardware requirements and to improve the reaction time of the 'machine protection system' in the case of device failures.

3 Collective effects

The intensity and quality of the beam in an accelerator are usually limited by collective effects. In the following, the characteristic effects and their peculiarities in the case of ERLs are discussed.

3.1 Space charge

Space charge effects typically limit the performance of the low-energy beam transport in high-brightness photoinjectors. One direct effect is transverse defocusing of the beam by space charge forces within bunches. The linear part of the forces can be compensated by external focusing (by solenoids or quadrupoles), but the non-linear part still affects the beam quality. Emittance degradation due to collective space charge forces is one of the important issues in the design of injector optics. Flat-top cathode laser profiles, both transversely and longitudinally, which linearize the space charge forces in the central part of the beam, are routinely used to achieve the highest beam brightness [1, 25].

If the aim is to achieve a high-brightness electron beam in an ERL, the injector should be designed with the emittance compensation technique [9] in mind. The critical difference between an ERL and a conventional linac injector is the merger section, where axial symmetry of the beam can no longer be assumed. This means that emittance compensation with a solenoid is not enough any more to achieve the minimum beam emittance in both planes. A theory of so-called '2D emittance compensation' was developed in Ref. [10]. The application of this method to the superconducting RF photoinjector in the bERLinPro project [5] is described in [26].

Space charge effects determine the choice of the merger geometry. An overview of practical merger designs can be found, for example, in Ref. [11]. One problem with a space-charge-dominated merger is the longitudinal space charge force, which affects the transverse motion of individual bunch slices in a dispersive section. Transverse defocusing and changes in the energy of a slice, caused by space charge forces, can modify the achromatic condition significantly. This effect favours merger designs that are short and have a low dispersion [26]. The linear part of the effect can be corrected if the bunch has a sufficiently large correlated energy spread.

Particle-tracking codes (e.g., Parmela [27], ASTRA [28], and GPT [29]) can be used to model space-charge-dominated beams. Usually, these programs require extensive resources for tracking, which

makes optimization of beam lines time- and resource-consuming. There are space charge codes (e.g., Trace3D [30], SCO [31], and HOMDYN [32]), which allow fast tracking of a model charge distribution (a Kapchinsky–Vladimirsky distribution, applied to a whole bunch or slicewise). These codes allow an initial optimization to be achieved quickly; afterwards, tracking with 'full' space charge codes can be done.

See specialized contributions in this CAS, especially "Space Charge Mitigation" (Massimo Ferrario, INFN-LNF).

3.2 Coherent synchrotron radiation

Although synchrotron radiation is usually emitted incoherently (i.e., ISR), very short electron bunches generate CSR with wavelengths comparable to the bunch length. The resulting energy loss can become very significant. For typical bunch lengths in storage rings (20–100 ps), CSR is shielded by the vacuum chamber and plays only a minor role in the beam dynamics. In linacs, however, where bunches can easily be compressed, CSR can strongly influence the beam parameters. Moreover, with the high average beam currents typical of ERLs, CSR can cause damage to vacuum system components as a result of its high average power. As an example [5], the CSR losses of bERLinPro in normal operation with 2 ps bunches and 100 mA average current were estimated to be 2.5 kW. For short-pulse operation mode at full current (100 mA) and with bunch lengths down to 150 fs, the losses would increase to about 25 kW.

The main problems and solutions related to the effects of CSR on the beam emittance have been investigated, for example, for short-wavelength FELs (FLASH, LCLS, and XFEL). If the key effect of the CSR wake on a bunch is a longitudinal-position-dependent transverse kick to the bunch slices, a 1D model can be a good approximation. A comprehensive derivation of 1D CSR wake functions for different cases is presented in [33]. This model has also been implemented in a number of packages (e.g, Elegant and Opal) [34, 35].

For very short bunches (if the bunch is, in its reference frame, equal in length to or shorter than its transverse sizes), the full 3D radiation field should be taken into account. Appropriate simulation codes (e.g., CSRTrack [36]) should be used in this case. However, the 1D model usually gives an overestimation of the effect and can still be used for quick checks.

CSR-induced emittance growth can be reduced by several methods. The increase in the transverse emittance is proportional to the $\mathcal{H}$-function (Eq. (1)), so keeping this function low reduces emittance degradation. In an ERL, this measure is essential in the magnets, where the bunches are at their shortest.

If the effect on the bunches is small, magnetic optics with a repetitive symmetry and an appropriate betatron phase advance between cells can cancel out the CSR kicks (see, e.g., [37] and references therein for the implementation of this method in FERMI@Elettra). The idea is easy to understand when the bunch length does not change along the beam line, so that the CSR emission conditions don't vary, i.e. with an isochronous arc or a bunch without correlated energy spread. In this case the energy change imprinted on every bunch slice is the same in each cell of the periodic focusing system. The final displacement and angle of the slice are the sums of the displacements and angles arising from each cell (i.e., a superposition). If the betatron phase advance from cell to cell is $2\pi k/N$, where k is any integer and N is the number of cells, then

$$\begin{pmatrix} x \\ x' \end{pmatrix} = \begin{pmatrix} x_1 \\ x'_1 \end{pmatrix} \sum_{k=1}^{N} \exp\left[2\pi i k/N\right] = 0 \ ,$$

i.e., all slices are aligned again.

A similar approach is possible even for a periodic arc with bunch compression. In this case the assumption of a self-similar CSR wake is necessary, which is not always satisfied. For example, the CSR wakes in the drifts are not self-similar. The implementation of such emittance correction is described, for example, in [7].

3.3 Microbunching instability

The average power coherently emitted from a short bunch is $P_{\text{total}} \sim Q_{\text{B}}^2/R^{2/3}\sigma_z^{4/3}$, and is capable of causing significant beam quality degradation. The effect can be greatly intensified if the bunch is structured on scales much shorter than the bunch length.

The mechanisms of such 'microbunching' can involve different wakes, the most important being those due to the longitudinal space charge (LSC) and the CSR itself [38–40]. The CSR wake shows only a weak dependence on the beam energy, whereas the LSC wake scales with $1/\gamma^2$ and therefore plays an important role in the low-energy, injector part of an accelerator. The wake imprints an energy modulation on the bunch, which can be transformed further into a longitudinal density modulation (microbunching). In a storage ring, the momentum compaction factor α_{c} and, in a linear accelerator, the element R_{56} of the transport matrix is responsible for this. This is the same matrix element that is necessary for bunch compression, so the two processes are intrinsically dependent on each other. The amplification factor of the density modulation (gain) in a beam line can be found, for example, in Ref. [40]. The initial density modulation can be imprinted in the RF photogun, for example by the longitudinal profile of the laser beam, which may be generated with a pulse shaper. Some details of the analysis that was done for LCLS can be found in Ref. [41]. Shot noise in the beam is another possibility, which usually gives a much lower initial modulation amplitude. The gain of this instability scales with the peak current of the bunch. An uncorrelated energy spread in the bunch smears out the bunching and can be used to suppress the instability [42]. A laser heater [43] is one option to increase the energy spread in a slice controllably; using a strong wiggler to induce an energy spread through emission of ISR is another.

3.4 Wakes and impedances

Resistive walls, surface roughness, and geometric wakes are other sources of distortions in ERL beam dynamics. Usually these distortions are smaller than those due to the CSR and LSC wakes. However, if countermeasures are taken to reduce or (ideally) completely compensate the effects of the CSR wake, they can become the main concern.

The resistive-wall impedance is usually higher for ERLs than for storage rings owing to the short bunch length achievable. The scaling is $k_{\text{L}} \sim \sigma_z^{-3/2}$ (for $\sigma_z > a/\gamma$), where k_{L} is the longitudinal loss factor, σ_z is the bunch length, a is the radius (half gap) of the vacuum chamber, and γ is the relativistic factor [44]. Surface roughness can also be an issue. For example, smooth NEG coating of the vacuum chambers may be necessary. Resonances in geometric wakes (when spectral lines of the beam coincide with resonances of the structure) should be avoided at the design stage, as was done, for example, for bERLinPro [45].

3.5 Linac configuration and beam break-up

Dipole-mode-driven transverse BBU can be a serious limitation in high-current operation of an ERL. This is primarily an ERL-specific problem, since accelerators that have high-quality-factor cavities (superconducting) and operate with a high average current are vulnerable to this instability.

Transverse BBU was observed and understood well at the JLab ERL [46]. A simple analytical scaling can be derived for the 'one cavity, one mode, one turn' case:

$$I_{\text{th}} = -\frac{2pc^2}{e\omega(R/Q)QR_{12}\sin(\omega T)}\ , \tag{5}$$

where I_{th} is the threshold current for the instability, p is the beam momentum, ω is the dipole mode frequency, $(R/Q)Q$ is the mode impedance, R_{12} is the element of the transport matrix of the recirculation, and T is the recirculation time. In the case of coupled optics and an arbitrary polarization angle α of the mode,

$$R_{12}^* = R_{12}\cos^2\alpha + (R_{14} + R_{32})\sin\alpha\cos\alpha + R_{34}\sin^2\alpha$$

has to be used instead of R_{12} [47]. The threshold current is proportional to the beam energy, so the most problematic cavities are those where the beam has its lowest energy. The threshold current for transverse BBU in the case of a single cavity and a single TM_{110} mode for a multipass ERL can be estimated as [48]

$$I_{\mathrm{b}} \approx I_0 \frac{\lambda^2/4\pi^2}{QL_{\mathrm{eff}}\sqrt{\sum\limits_{m=1}^{2N-1}\sum\limits_{n=m+1}^{2N}(\beta_m\beta_n/\gamma_m\gamma_n)}},$$

where I_0 is the Alfvén current, Q is the quality factor of the HOM, λ is the wavelength corresponding to the resonant frequency of the mode, γ_m is the relativistic factor at the mth pass through the cavity, β_m is the Twiss parameter, L_{eff} is the effective length of the cavity, and N is the number of acceleration passes. This expression indicates the limitation on the number of passes and suggests an optical design with beta functions as low as possible for cavities with low beam energy.

As was shown in Ref. [49], the BBU threshold current for an N-turn ERL may be estimated as roughly $N(2N-1)$ times smaller than that for a single-turn machine. The worst-case scenario, where the betatron phase advances between all pairs of passes through the cavity were $\sin(\mu_{nm}) = 1$, was assumed in that estimate. The expression in Ref. [48] gives another estimate, assuming random phases, which is closer to reality for a 'large' number of cavities and passes. Numerical modelling of the transverse BBU instability is necessary to take many linac cavities into account, with all relevant modes. A number of codes for this purpose exist [50–52]. Also, a high arc chromaticity has been proposed as a measure to stabilize the beam against transverse BBU [53].

Longitudinal BBU driven by monopole modes is another issue for ERLs. In this case the longitudinal dispersion R_{56} replaces R_{12} in the estimate of the threshold current in Eq. (5) (see, e.g., [54]). If a single-turn ERL operates with $R_{56} = 0$, it is not vulnerable to this instability (at least in theory). However, in a multiturn ERL with bunch compression in the arcs, $R_{56} \neq 0$ and an analysis of this instability becomes necessary.

3.6 Ion trapping

ERLs are vulnerable to the effects of ions accumulated in the potential well of the electron beam. These effects include:

- optical errors due to strong focusing of the electron beam by the space charge of the ion cloud;
- higher electron-beam scattering rates, leading to the formation of a beam halo and increased beam losses;
- ion-induced beam instabilities.

The ions are produced by electron ionization of the residual gas (ionization by synchrotron radiation is also possible). Confined inside the 'time-averaged electrostatic potential' of the electron beam, ions can be 'trapped' in the beam for a relatively long time, oscillating near the minima of the potential. These minima coincide with the minima of the beam size for axially symmetrical beams.

Simulation of the formation and dynamics of the ion cloud is complicated by the complex trajectories of ions in the potential of a non-axisymmetric electron beam and the fact that the dynamic equilibrium that determines the neutralization factor of the electron beam is defined by a competing process of ion heating (by scattering from the electrons). Modelling of these processes is therefore a complex task; some results can be found, for example, in Ref. [55]. The methods for clearing ions in an ERL are basically the same as those used in storage rings. Clearing electrodes, gaps in the bunch train, and resonant excitation of the ion cloud are discussed, for example, in [56, 57]. For small-scale machines, a gap is not a good option owing to the short recirculation time. The variable beam loading due to the fluctuating beam current is a general concern.

References

[1] S.J. Russell, *Nucl. Instrum. Methods Phys. Res. A* **507**, Issues 1-2, p. 304-309, (2003).

[2] A. Arnold and J. Teichert, *Phys. Rev. ST Accel. Beams* **14** (2011) 024801. https://doi.org/10.1103/PhysRevSTAB.14.024801

[3] http://journals.aps.org/prstab/.

[4] http://www.jacow.org/.

[5] Conceptual design report, bERLinPro, edited by B. Kuske, N. Paulick, A. Jankowiak, and J. Knobloch (2012).

[6] M. Abo-Bakr *et al.*, Progress report of the Berlin energy recovery project bERLinPro, Proc. IPAC15, Richmond, VA, 2015.

[7] T. Atkinson, A. Bondarenko, A. Matveenko, and Y. Petenev, 'Conceptual design report for a multi-turn energy recovery linac-based synchrotron light facility (femto-science factory) (Helmholtz-Zentrum Berlin, 2015), Section 5.2.3. https://doi.org/10.5442/R0002

[8] H. Wiedemann, *Particle Accelerator Physics* (Springer, 1993). https://doi.org/10.1007/978-3-662-02903-9

[9] L. Serafini and J. Rosenzweig, *Phys. Rev. E* **55** (1997) 7565. https://doi.org/10.1103/PhysRevE.55.7565

[10] S.V. Miginsky, *Nucl. Instrum. Methods Phys. Res. A* **603** (2009) 32. https://doi.org/10.1016/j.nima.2008.12.124

[11] V.N. Litvinenko, R. Hajima, and D. Kayran, *Nucl. Instrum. Methods Phys. Res. A* **557** (2006) 165. https://doi.org/10.1016/j.nima.2005.10.065

[12] J. Rosenzweig and L. Serafini, *Phys. Rev. E* **49** (1994) 1599. https://doi.org/10.1103/PhysRevE.49.1599

[13] Y. Petenev, Dissertation, HU Berlin, 2014.

[14] R. Hajima, *Nucl. Instrum. Methods Phys. Res. A* **557** (2006) 45. https://doi.org/10.1016/j.nima.2005.10.050

[15] R. Chasman *et al.*, Preliminary design of a dedicated synchrotron radiation facility, Proc. PAC 1975, Washington, DC, 1975.

[16] H. Owen and B. Muratori, Choice of arc design for the ERL prototype at Daresbury Laboratory, Proc. EPAC 2004, Lucerne, Switzerland, 2004.

[17] J.B. Flanz *et al.*, An isochronous beam recirculation magnet system, Proc. PAC 1981, Washington, DC, 1981.

[18] D. Trbojevic *et al.*, ERL with non-scaling fixed field alternating gradient lattice for eRHIC, Proc. IPAC'15, Richmond, VA, 2015.

[19] D. Trbojevic *et al.*, Lattice design for the future ERL-based electron hadron colliders eRHIC and LHeC, Proc. PAC11, New York, 2011.

[20] E. Jensen *et al.*, Design study of an ERL test facility at CERN, Proc. IPAC'14, Dresden, Germany, 2014.

[21] E. Cruz-Alaniz *et al.*, Tracking studies in the LHeC lattice, Proc. IPAC15, Richmond, VA, 2015.

[22] E.C. Aschenauer *et al.*, eRHIC design study: An electron–ion collider at BNL. https://arxiv.org/abs/1409.1633.

[23] A. Piwinski, The Touschek effect in strong focusing storage rings. https://arxiv.org/abs/physics/9903034.

[24] S.Y. Lee, *Phys. Rev. E* **54** (1996) 1940. https://doi.org/10.1103/PhysRevE.54.1940

[25] F. Stephan *et al.*, *Phys. Rev. ST Accel. Beams* **13** (2010) 020704. https://doi.org/10.1103/PhysRevSTAB.13.020704

[26] A.V. Bondarenko and A.N. Matveenko, Emittance compensation scheme for the bERLinPro injector, Proc. IPAC'11, San Sebastian, Spain, 2011.

[27] L.M. Young and J.H. Billen, PARMELA documentation, LA-UR-96-1835, Los Alamos National Laboratory, Revised April 18, 2005.

[28] K. Floettmann, ASTRA: A space charge tracking algorithm, http://www.desy.de/ mpyflo/.

[29] S.B. van der Geer *et al.*, GPT: The general particle tracer, http://www.pulsar.nl/gpt.

[30] D. Rusthoi, W. Lysenko, and K. Crandall, Further improvements on trace 3-D, Proc. PAC (1997), Vancouver, B.C., Canada.

[31] A.V. Bondarenko and A.N. Matveenko, Implementation of 2D-emittance compensation scheme in the bERLinPro injector, Proc. FEL 2011, pp. 564–567, Shanghai, China.

[32] M. Ferrario, HOMDYN user guide, SLAC 3/1/02 (1999).

[33] E.L. Saldin, E.A. Schneidmiller, and M.V. Yurkov, *Nucl. Instrum. Methods Phys. Res. A* **398** (1997) 373. https://doi.org/10.1016/S0168-9002(97)00822-X

[34] M. Borland, *Phys. Rev. ST Accel. Beams* **4** (2001) 070701. https://doi.org/10.1103/PhysRevSTAB.4.070701

[35] https://amas.psi.ch/OPAL.

[36] M. Dohlus and T. Limberg, CSRTrack user manual, http://www.desy.de/xfel-beam/csrtrack/.

[37] S. Di Mitri, M. Cornacchia, and S. Spampinati, *Phys. Rev. Lett.* **110** (2013) 014801. https://doi.org/10.1103/PhysRevLett.110.014801

[38] G. Stupakov, Theory and observations of microbunching instability in electron machines, SLAC-PUB-9880 (2003).

[39] G. Stupakov and S. Heifets, *Phys. Rev. ST Accel. Beams* **5** (2002) 054402. https://doi.org/10.1103/PhysRevSTAB.5.054402

[40] Ya.S. Derbenev, J. Rossbach, E.L. Saldin, and V.D. Shiltsev, Microbunch radiative tail–head interaction, Deutsches Elektronen-Synchrotron Report No. TESLA-FEL 95-05 (1995).

[41] J. Wu *et al.*, Temporal profile of the LCLS photocathode ultraviolet drive laser tolerated by the microbunching instability, SLAC-PUB-10430 (2004).

[42] S. Heifets *et al.*, *Phys. Rev. ST Accel. Beams* **5** (2002) 064401. https://doi.org/10.1103/PhysRevSTAB.5.064401

[43] Z. Huang *et al.*, *Phys. Rev. ST Accel. Beams* **7** (2004) 074401. https://doi.org/10.1103/PhysRevSTAB.7.074401

[44] A. Chao and M. Tigner (Eds.), *Handbook of Accelerator Physics and Engineering* (World Scientific, Singapore, 1999).

[45] H.-W. Glock *et al.*, Loss factor and impedance analysis of warm components of bERLinPro, Proc. IPAC15, Richmond, VA, 2015.

[46] C. Tennant *et al.*, *Phys. Rev. ST Accel. Beams* **8** (2005) 074403. https://doi.org/10.1103/PhysRevSTAB.8.074403

[47] E. Pozdeyev, *Phys. Rev. ST Accel. Beams* **8** (2005) 054401. https://doi.org/10.1103/PhysRevSTAB.8.054401

[48] N.A. Vinokurov *et al.*, *Proc. SPIE* **2988** (1997) 221. https://doi.org/10.1117/12.274385

[49] G.H. Hoffstaetter and I.V. Bazarov, *Phys. Rev. ST Accel. Beams* **7** (2004) 054401. https://doi.org/10.1103/PhysRevSTAB.7.054401

[50] E. Pozdeyev *et al.*, *Nucl. Instrum. Methods Phys. Res. A* **557** (2006) 176. https://doi.org/10.1016/j.nima.2005.10.066

[51] I. Bazarov, bi—beam instability BBU code. http://www.lepp.cornell.edu/ ib38/bbu/

[52] L. Merminga and I.E. Campisi, Higher-order-models and beam breakup simulations in the Jefferson Lab FEL recirculating linac, 19th International Linear Accelerator Conference, 1998.

[53] V.N. Litvinenko, *Phys. Rev. ST Accel. Beams* **15** (2012) 074401. https://doi.org/10.1103/PhysRevSTAB.15.074401

[54] J. Bisognano and M. Fripp, Requirements for longitudinal HOM damping in superconducting linacs, CEBAF-PR-89-018, 1989.

[55] G. Pöplau, U. van Rienen, and A. Meseck, *Phys. Rev. ST Accel. Beams* **18** (2015) 044401. https://doi.org/10.1103/PhysRevSTAB.18.044401

[56] G.H. Hoffstaetter and M. Liepe, *Nucl. Instrum. Methods Phys. Res. A* **557** (2006) 205. https://doi.org/10.1016/j.nima.2005.10.069

[57] S. Full *et al.*, Detection and clearing of trapped ions in the high current Cornell photoinjector. http://arxiv.org/pdf/1508.00923.pdf